Accounting for turbulence in gas explosion venting design

Jérôme Daubech, Emmanuel Leprette, Audrey Duclos, Christophe Proust

Accounting for turbulence in gas explosion venting design

Jérôme Daubech [a], Emmanuel Leprette [a], Audrey Duclos [b] & Christophe Proust [a,b]

E-mail: *jerome.daubech@ineris.fr*

[a] Institut National de l'Environnement Industriel et des Risques, Parc Technologique ALATA, BP 2, 60550 Verneuil-en-Halatte, France
[b] Sorbonne Universités, UTC-TIMR, 1 rue Dr Schweitzer, 60200 Compiègne, France

Abstract

With the publication of NFPA 68 (2013); a major change is in progress in venting area calculation methods for gas explosions. Old methods referring to the Kg parameter proved to be inappropriate for real applications.

The present work provides new data to correlate real gas concentration and initial turbulence conditions to flame propagation and explosion overpressure during a vented gas explosion. Explosion tests were performed in a 4 m^3 rectangular chamber equipped with transparent walls and vented (0.49 m^2 square vent) on one side. The chamber is filled with a turbulent or quiescent hydrogen-air mixture with a purposely built injection system that allows to vary the turbulence intensity and the length scale. Gas concentration and turbulence parameters are measured with concentration gauges and Pitot probes distributed in the chamber (Duclos, 2017). Then the flame propagation is fully characterized with high speed video and explosion overpressure is measured inside and outside the chamber. The paper presents the parametric study performed by varying the initial turbulence and focuses on its influence on the inside explosion overpressure. Then physics of vented gas explosion is discussed, results are compared to developing phenomenological model.

Keywords: *mitigation, gas explosion, vented explosion, turbulence, venting design*

1 Introduction

An important effort was made during the second part of the 20th century to develop models able to calculate accurately the venting area. These phenomenological models try to take into account a number of physical phenomena like the evolution of the flame shape as function of the geometry of the vessel (Bradley et al, 1978, Wu et al., 1996), the hydrodynamic instabilities (Puttock et al. 1996), the turbulence of the flow ahead of the flame (Cates,1991), the characteristics of the vent cover: inertia, discharge coefficient … (Molkov, 2003). Although they become more and more predictive, these analytical and phenomenological models cannot be generalized to all the situations (Jallais, 2013), suggesting several phenomena may not yet be well understood or correctly accounted for.

A set of papers (Van Wingerden, 1983, Cooper, 1986, Bimsom, 1993) suggest that flame instabilities or different nature (Taylor, hydrodynamic, acoustic...) play a great role and that in particular the external combustion of the cloud in front of the vent (Chow, 2000, Harrison, 1987, Catlin, 1991) interacts strongly with the internal explosion. In fact, the degree of interaction is prevailing especially at large scale with large "vent" ratios (Proust, 2010).

Moreover, very few experimental works are dedicated to study the influence of initial turbulence on vented explosion dynamics. Bauwens (2014) performed experiments examining the effect of initial low level of turbulence generated by fans on vented propane-air and hydrogen-air explosions. He observed that an increase in initial turbulence increases the flame propagation speed and the maximum overpressure during the external explosion.

The paper presents the parametric study performed by varying the initial turbulence and focuses on its influence on the inside and outside explosion overpressure and the physics of vented gas explosion is discussed.

2 Experimental set-up and instrumentation

2.1 Experimental set-up

The experimental installation (Figure 1) consists of:

- A 4-m^3 enclosure
- A pressurized 50 L tank containing the flammable gas equipped with three electro-pneumatic valves; for the gas supply , for the purge and for the injection in the enclosure ;
- An isolation valve to isolate the tank from the enclosure;
- A seeding system to render the cloud optically thick and visualize the flame front propagation;
- A gas dispersionsystem in the enclosure.

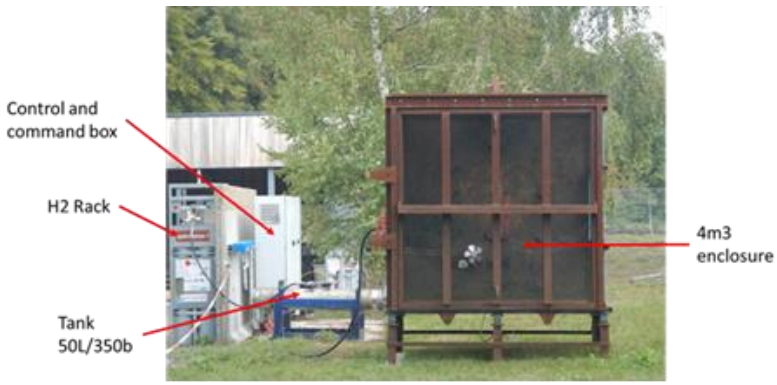

Figure 1: Illustration of the experimental set-up

The 4-m^3 enclosure is 2-m length, 2-m height and 1-m width. It comprises three transparent walls, a vent located (1.6 m above the floor) on a lateral wall and centered on the horizontal axis of the vessel. The mechanical resistance of of the mock-up is provided by a network of T-iron beams and I-iron beams (50 mm thick) supporting the transparent faces (2-cm-

thickness PMMA). The other walls (not transparent) are 5-mm-thickness plates of steel mechanically reinforced by 5-mm I-iron beams (Figure 2).

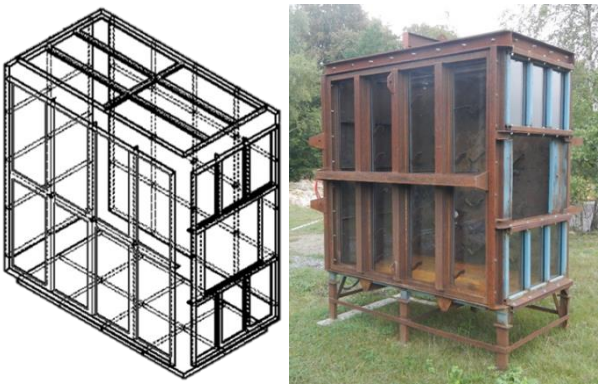

Figure 2: Assembly and picture of the experimental mock-up

The 50 L tank (Figure 3) is made of 316L stainless steel (adapted to hydrogen) and withstands a pressure up to 350 bars. It is equipped with three electro-pneumatic valves; for the gas supply, for the purge and for the injection in the enclosure. The tank is also equipped with a thermocouple and a pressure sensor to obtain all the data to calculated the mass flow rate.

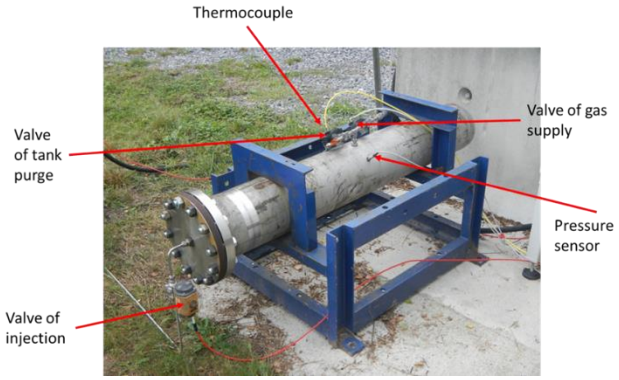

Figure 3: Tank of discharge

The gas is injected at the centre of the floor of 4m^3 chamber by discharging the 50 L tank through a circular hole (diameters: 1 and 3 mm). The vent is covered by a plastic sheet maintained by magnetic bands to contain the flammable cloud during the injection and before ignition.

2.2 Instrumentation

The concentration distribution is measured with 6 oxygen analyzers sampling the atmosphere along the vertical axis every 35 cm. The Pitot sensors (Proust, 2018) are connected to differential pressure transducers Texence DPS-70-2.5. The flow velocity is derived from the difference of dynamic pressure, and then the turbulence intensity *u'* comes from the flow velocity fluctuations around the mean value $\bar{u}$:

$$u' = \sqrt{\frac{1}{n}\sum_{i=1}^{n}(u_i - \bar{u})^2} \text{ with } \bar{u} = \frac{1}{n}\sum_{i=1}^{n} u_i$$

To measure the integral scale, the original Pitot sensor had been replaced by bended capillaries connected to the positive port of the differential pressure sensors. All the second ports of the differential pressure sensors are exposed to the atmospheric pressure. The turbulence integral length is calculated using the spatial correlation. More details on dispersion instrumentation and experiments are presented by Duclos (2017).

To make the flammable cloud and the propagating flame visible, the mixture is seeded with ammonium chloride microparticles during the preparation of the mixture. To do so, ammonia vapors and hydrochloric acid contained in two different tubes are mixed to produce fine particles of ammonium chloride which are injected in the chamber. This technique does not modify the flammable mixture reactivity and the flame behavior (Daubech, 2008). The vent area (0,49 m^2) is covered with a very thin plastic sheet held with magnetic tapes. Ignition is achieved using an electrical spark (100 mJ).

Two piezoresistive gauges (KISTLER 0-10 bar accuracy ± 0.1 %) are used to measure the pressure evolution inside (Figure 4). The first gauge (P1) is located on the small side opposite to the vent, the second one (P2) is in the center of the large side opposite to the front transparent wall. Four additional piezoresistive gauges (KISTLER 0-2 bar accuracy ± 0.1 %) are used to measure the pressure evolution outside. Two pressure gauges are located on the axis of the vent at 2 m and 5 m from the vent. The other two stands perpendicularly at 2 m and 5 m from the axis of the vent aligned with the vent. The cloud formation in front of the vent and the flame propagation are filmed using a high-speed video camera (PHOTRON Fastcam).

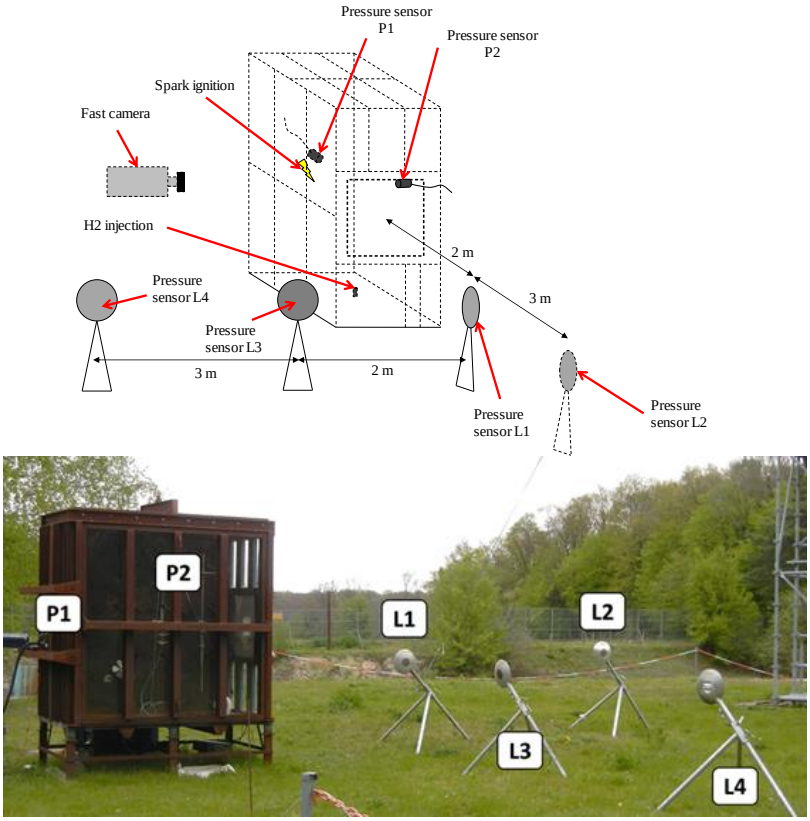

Figure 4: Explosion instrumentation

3 Experiments

The dispersion works had been already presented by Duclos (2017). The explosion tests are performed in the same conditions as the dispersion. Three concentrations are tested: 10%; 16%; and 21% vol. of hydrogen in air. Those concentrations are obtained by varying the initial pressure in the tank; the release orifice diameter and the release duration. The transition from a "quiet atmosphere" configuration to a "turbulent atmosphere" configuration comes about reducing the delay between the end of the injection and the ignition, passing from 15 s to 200 ms. Analysis of a typical test

A phenomenological analysis of a typical experiment with a uniform and quiet atmosphere at 16% vol. of hydrogen; is detailed in this paragraph. In Figure 5 the internal and external overpressure's signals and pictures extracted from the video of the high-speed-camera are represented.. This test is similar to those presented by Daubech (2013).

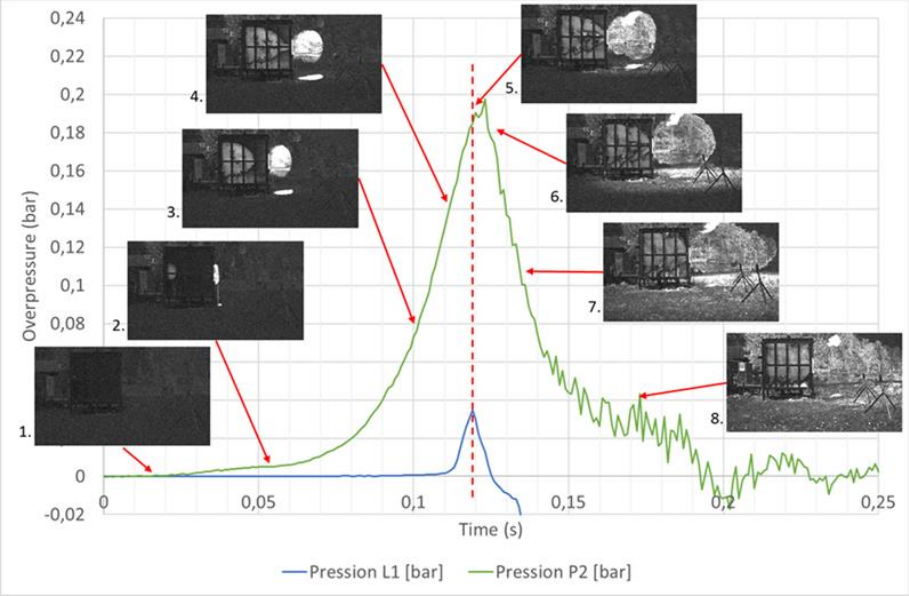

Figure 5: Internal and external overpressure's signals and pictures extracted from the high-speed-camera for homogeneous and quiescent 16% hydrogen-air mixture, rear ignition, square vent surface: 0.49 m^2

The explosive atmosphere inside the enclosure is ignited at the back wall ("rear ignition" Picture 1 on Figure 5). The flame propagates from the ignition point to the vent. Just after the ignition (Picture 2 on Figure 5), the flame develops as an hemisphere around the ignition point and its borders are clearly well defined. At the same time, a part of the reactant gases starts being expelled outside the enclosure. The expelled gases form a vortex cloud having a radius on the same order of magnitude than the vent diameter (Picture 3 on Figure 5). At the same time, the flame continues to propagate in the enclosure and the pressure continues to increase too. The flame seems to take a half-ellipsoid form, as already observed by Catlin (1991). The borders of the flame stay well defined. The external cloud is ignited by the flame rushing out of the enclosure at around 110 ms (Picture 4 on Figure 5). At this time, part of the reactant gases starts being expelled outside the enclosure. The expelled gases form a vortex cloud having a radius on the same order of magnitude than the vent diameter (Picture 3 on

Figure 5). At the same time, the flame continues to propagate in the enclosure and the pressure continues to increase. The flame resembles a half-ellipsoid, as previously observed by Catlin (1991). The borders of the flame stay well defined. The external cloud is ignited by the flame rushing out the enclosure at about 110 ms (Picture 4 on Figure 5). At this moment, the internal overpressure is 0.12 bar. Then the flame propagates into the external cloud and generates an external explosion /secondary explosion (Picture 5 on Figure 5). At this moment, the internal combustion is not finished and the internal overpressure is 0.187 bar. The external explosion (Picture 5 and Picture 6 on Figure 5) produces a pressure wave propagating in the surrounding. This external explosion is also responsible for a small re-pressurization in the enclosure due to the blockage of the flow through the vent and the internal overpressure reaches its maximum, 0.197 bar. After the external explosion, the rest of the flammable mixture in the enclosure continues to burn and the hot combustion products are discharged through the vent as a hot jet (Picture 7 on Figure 5).

Figure 6 presents the axial flame velocity versus the flame position. The flame propagates with a uniformly accelerated motion up to 1.3 m from the ignition point. The acceleration factor is about 330 m/s2. The average flame velocity in this first part of propagation is around 15 m/s. After, the flame accelerates before going out. The flame accelerates on the last 0.7 m. This distance corresponds to the characteristic dimension of the vent. This last acceleration phase is related to the accelerated flow field through the vent.

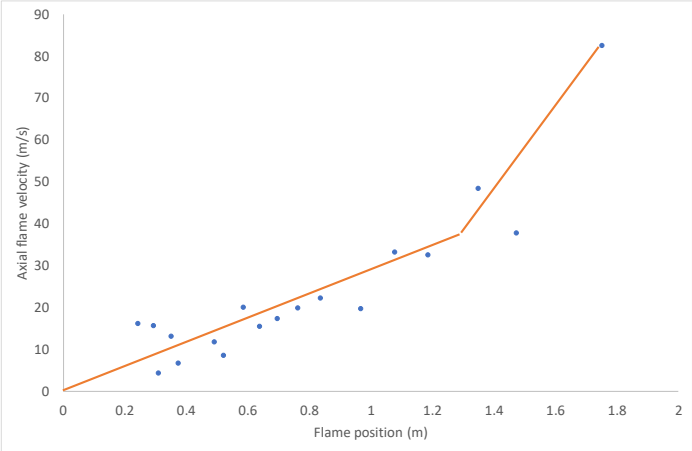

Figure 6: Axial flame velocity versus flame position for homogeneous and quiescent 16% hydrogen-air mixture, rear ignition

This flame acceleration at 1.3 m appears also for quiescent homogeneous mixtures of 10 and 21 % vol of H_2 in air.

The external cloud is ignited when the flame, rushing out of the vent, reaches the stagnation point at the leading edge of the vortex. Then the flame is wrapped very fast around the vortex ring and the maximum expansion velocity of the burning cloud occurs at this moment (Figure 5) in typically 12 ms (110-122 ms). The maximal extension of the external cloud (1.4 m) is twice as great as the characteristic dimension of the vent, the average burning velocity of the vortex is about 115 m/s.

Table 1 presents a summary of results for 10, 16 and 21 % vol H2 in air quiescent homogeneous mixtures:

- Inside average flame velocity,
- Maximum overpressure inside the enclosure,
- Time of flame exit,
- Duration of external combustion,
- Outside average flame velocity.

Expansion ratio and laminar burning flame velocity for the three mixtures come from Koroll (1994).

Table 1: Summary of results for 10, 16 and 21 % vol H2 in air quiescent homogeneous mixtures.

Concentration of hydrogen	Expansion Ratio E	Laminar burning velocity Slad (m/s)	Theoretical flame velocity E.Slad (m/s)	Inside average flame velocity (m/s)	Maximum Overpressure (bar)	Time of flame exit (ms)	Duration of external combustion (ms)	Outside average flame velocity (m/s)
10 %	3.4	0.3	1.	9	0.040	237	73	20
16 %	4.9	1.1	5.4	15	0.200	110	12	115
21 %	5.9	1.7	10	30	0.430	63	10	140

The theoretical flame propagation velocity $E.S_{lad}$ is smaller than the inside average flame velocity by a factor 3 for 16 % and 21 % H_2-air mixtures and a factor 9 for 10% H_2-air mixtures. This factor suggests that flame is accelerated by hydrodynamic instability.

3.1 Influence of turbulence on overpressure and flame propagation

The selected situation is the 16 % H_2/air turbulent mixture created by the discharge of the 40 bar pressurized tank through a 3 mm hole. The discharge duration is 8 s. The average intensity of turbulence u' and the average turbulence length scale L_t measured for this release in the 4 m^3 chamber are respectively 5.5 m/s and 7 cm.

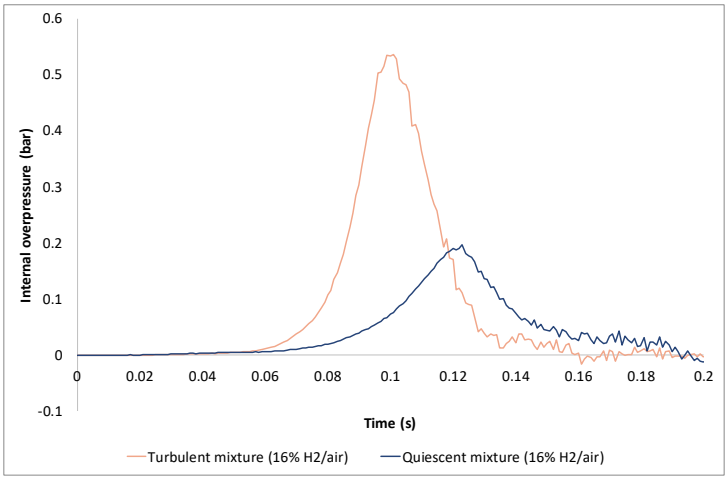

Figure 7: Internal pressure signals – homogeneous 16 % H_2/air turbulent and quiescent mixtures, rear ignition, square vent surface: 0.49 m^2

For the 16% H_2-air turbulent mixture, the maximum overpressure is reached at 100 ms and is equal to 0.535 bar. There is a factor 2,5 between overpressures for quiescent and turbulent mixtures.

The average flame propagation velocity is about 60 m/s according to the high-speed video.

Table 2 presents the value of average flame velocity for 10 %, 16 % and 21 % for turbulent mixtures in the same initial conditions of discharge (initial pressure tank: 40 bar, release hole diameter: 3 mm), the turbulence conditions and the maximum internal overpressure.

Table 2: Turbulence characteristics (u' and Lt), average flame velocity and maximum overpressure for 10 %, 16 % and 21 % for turbulent mixtures

Concentration of hydrogen	u' (m/s)	Lt (cm)	Average flame velocity turbulent mixture (m/s)	Maximum internal overpressure (bar)
10 %	7	7	25	0.265
16 %	5.5	7	55	0.535
21 %	5	7	60	0.805

4 Discussion

Thanks to these experimental data and the previous INERIS works, it is possible to develop a phenomenological model to estimate the flame velocity for quiescent and turbulent mixture and the inside overpressure.

4.1 Estimation of flame velocity

It is possible to estimate the flame propagation velocity thanks to the "generalized" model of Taylor (Daubech, 2008). This model accounts for the influence of the hydrodynamics instabilities, caused by the density gradient through the flame front and the "Taylor" instabilities generated by the flow acceleration.

Naturally, a flame that propagates in a homogenous quiescent mixture perfectly is covered in "bubbles" under the effect of Landau-Darrieus "hydrodynamic" instabilities, but it turns out that this mechanism is self-limiting and that apparent combustion speed can be estimated by:

$$U_{LD} = \left[1 + 4E * \frac{(E-1)^2}{(E^3 + E^2 + 3E - 1)}\right] * S_{lad} = \delta_{LD} * S_{lad}$$

However, if the flame velocity is submitted to Rayleigh-Taylor instabilities caused by a variation of the flow velocity (due to turbulence for example), the flame velocity U_{RT} can be estimated with the following equation:

$$U_{RT} = 0.51 * \sqrt{\left(\frac{E-1}{E} * \eta_{acc} * r\right)}$$

Where E is the expansion ratio, S_{lad} the laminar burning velocity, η_{acc} the acceleration of the flow and r the flame curvature.

Finallyn the combustion velocity U_{comp} results from the contribution of the two instabilities U_{LD} and U_{RT}.

$$U_{comp} = \sqrt{U_{RT}^2 + U_{LD}^2}$$

For the "Taylor" instabilities, the acceleration term can be expressed as a function of the mechanism that leads to it. In case of a turbulent flow, the acceleration has typically the same order of magnitude as the $\eta_{acc} = {u'^2}/{L_t}$.

For the experimental work presented in this paper, the flame curvature is equal to 1 m (half the height of the enclosure). Figure 8 presents a comparison between the experimental flame velocity, the laminar burning velocity multiplied by the expansion ratio *E*. S_{lad} and U_{comp} multiplied by the expansion ratio. For quiescent and turbulent mixture, the agreement seems quite reasonable.

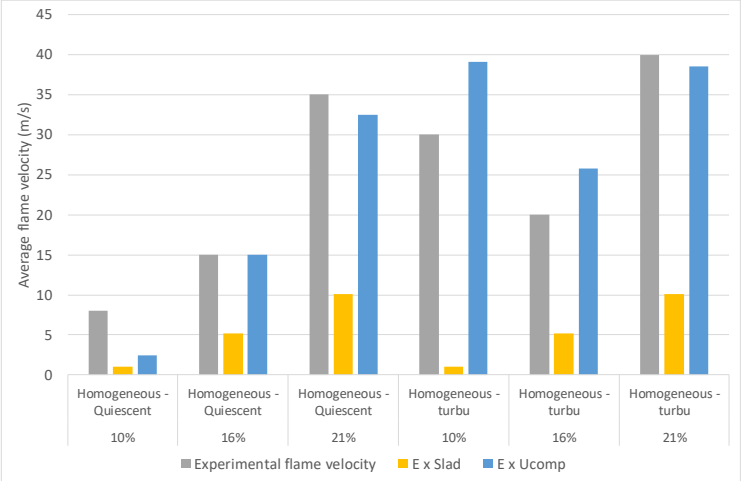

Figure 8: Comparison between the experimental flame velocity, the laminar burning velocity multiplied by the expansion ratio and U_{comp} multiplied by the expansion ratio.

4.2 Correlation between overpressure and flame velocity

As already established by Lewis and Von Elbe (1987), the maximum overpressure in the enclosure is correlated to the average flame velocity. For the 4m^3 chamber with a square vent of 0.49 m^2, the dependence between overpressure and average flame velocity looks linear (Figure 9).

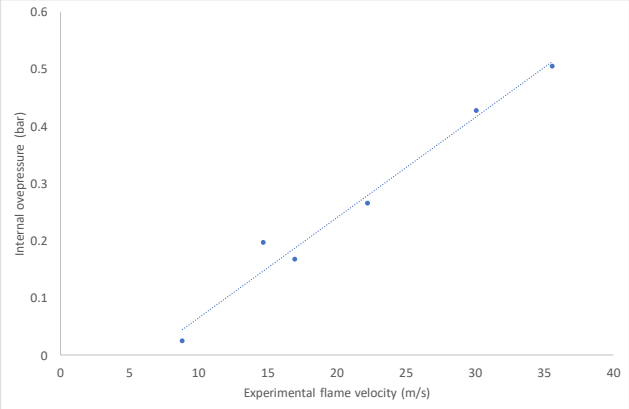

Figure 9: Overpressure in the enclosure in function of the experimental flame velocity

It's possible to develop an iterative phenomenological model to evaluate the overpressure evolution in time in the 4 m^3 enclosure regarding the geometrical evolution of flame. The classical theory of flame propagation in enclosure is used (Lewis and Von Elbe, 1987). The evolution of internal overpressure ΔP is estimated by a balance between the production flow rate of burnt gases by the flame Q_{flm} and the unburnt gas flow rate expelled by the vent until the flame rushes out the enclosure:

$$\frac{1}{\Delta P(t)}\frac{d(\Delta P(t))}{dt} = \gamma.\frac{Q_{flm}(t) - Q_{ouv}(t)}{V}$$

With $$Q_{flm}(t) = S_t.A_f(t).(E-1).\frac{\rho_U.P_0}{\rho_{U0}.P} \qquad Q_{ouv}(t) = -C_d.A_v.f(\Delta P(t))$$

Where V is the volume of the enclosure, A_f is the flame area, A_v is the vent area, S_t is the turbulent combustion velocity, ρ_{u0} is density of unburnt gases, P_0 is the initial pressure in the chamber and f(ΔP) is a function of internal overpressure (calculated at each time step).

The flame area is approximated by a half ellipsoid for which:

- the half major axis of the ellipsoid moves with a velocity calculated by the "generalized" model of Taylor risen by the flow velocity when the flame comes neat the vent,
- the half minor axis moves with flame velocity equal to $E.S_{lad}$ for quiescent mixtures, $E.U_{comp}/\delta_{LD}$ for turbulent mixtures.

The flame velocity of external cloud is determined by the experimental relation published by Proust (2010) where the maximal flame ball expansion velocity V_{ex_flame} is directly correlated to the flow velocity at the vent V_{flow_vent} thanks to:

$$V_{ex\_flame} = 8.3853\ (V_{flow\_vent})^{0.5223}$$

with $V_{flow\_vent} = \sqrt{\frac{2.\Delta P}{\rho}}$ where ΔP is the internal overpressure before the exit of the flame and ρ the density of the reactants

The external overpressure in the vortex is calculated by the Lannoy relation $\Delta P_{\exp-cloud}(t) \approx \frac{3}{2} \cdot \rho_{atm} \cdot V^2_{ex\_flame}(t)$ and the contribution of external overpressure on internal overpressure is proportional to the ratio of venting area and cross section of the enclosure.

Figure 10 presents comparison between internal and estimated overpressure by the model for homogeneous quiescent and turbulent mixtures of 16% and 21% hydrogen in air (initial tank pressure = 40 bar, release hole diameter = 3 mm, square vent = 0,49 m^2, rear ignition). Despite the time offset, the model reproduces correctly the dynamic of pressure rise-up and estimates the maximum overpressure with a difference of less than 10 %.

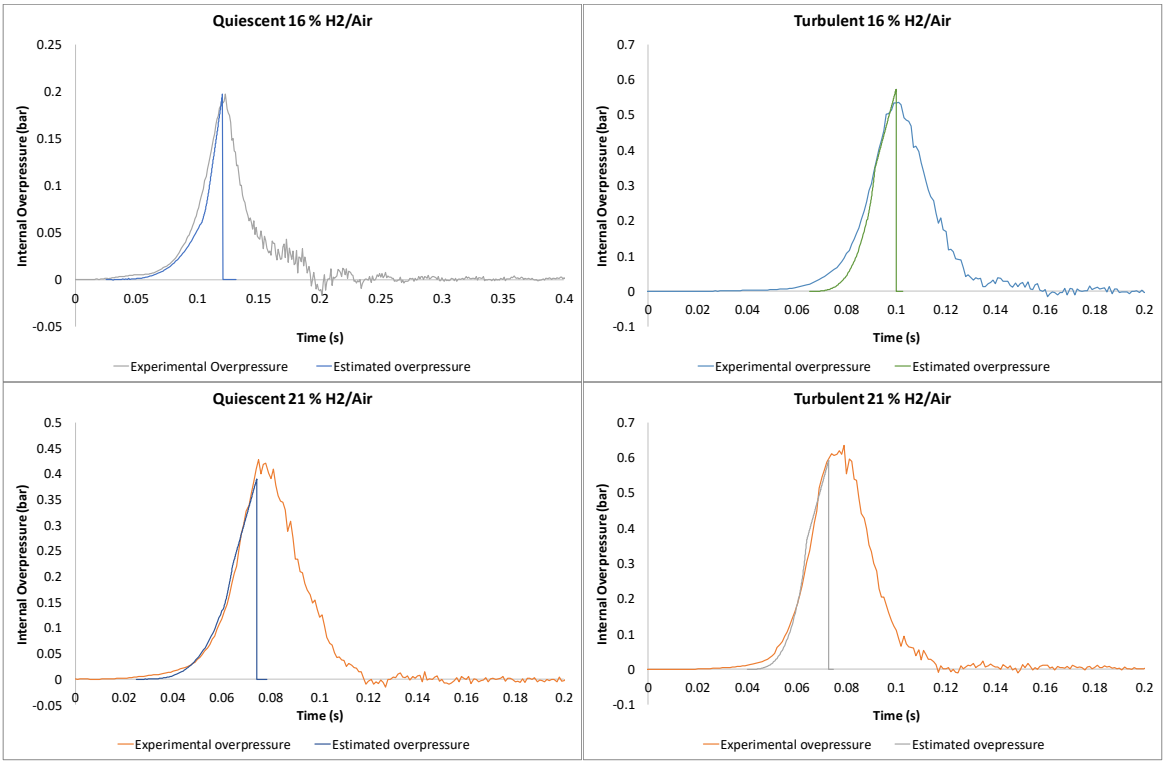

Figure 10: Comparison between internal and estimated overpressure by the model for homogeneous quiescent and turbulent mixtures of 16% and 21% hydrogen in air (initial tank pressure = 40 bar, release hole diameter = 3 mm, square vent = 0,49 m^2, rear ignition)

5 Conclusions

This present work provides a set of new experimental data which correlates real gas concentration and turbulence initial conditions to flame propagation and explosion overpressure during a vented gas explosion. The work of analysis is keep on going.

A phenomenological model is implemented. It is based on the "generalized" model of Taylor, the balance between the production flow rate of burnt gases by the flame and the unburnt gas flow rate expelled by the vent and the experimental INERIS correlation for external combustion. A specific effort will be made to better understand the combustion of external vortex and replace the experimental correlation with a physical law. However, this model is confronted to Bauwens (2012) larger experiments: vented deflagrations in 64 m^3 chamber equipped with 2,7 m^2 or 5,4 m^2 vent areas from lean H_2/air flammable mixtures – rear ignition. Presents a comparison for experimental and estimated reduced overpressures.

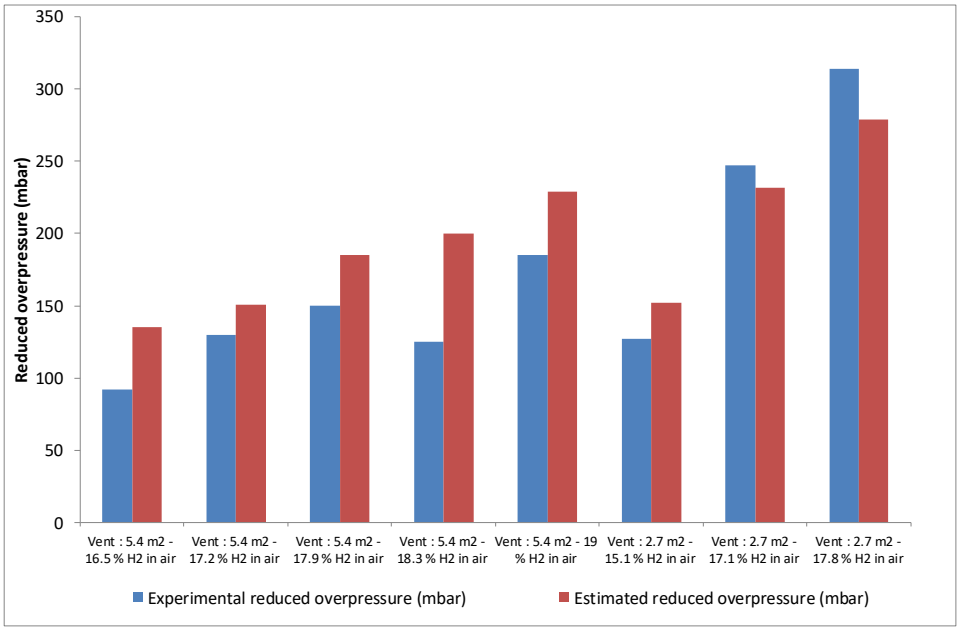

Figure 11 : Comparison for experimental and estimated reduced *over*pressures - vented deflagrations in 64 m3 chamber equipped with 2,7 m2 or 5,4 m2 vent areas from lean H2/air flammable mixtures – rear ignition

References

NFPA (2002), *Venting of deflagrations*, NFPA 68, USA

BRADLEY D., MITCHESON A. (1978), *The venting of gaseous explosions in spherical vessels I-theory*, Comb. and Flame, vol. 32, pp. 231-236

WU Y., SIDDALL R.G. (1996), *A mathematical model for vented explosions in a cylindrical chamber*, TransIChemE, vol. 74, part B, pp. 31-37

PUTTOCK J.S., CRESSWELL T.M., MARKS P.R., SAMUELS B., PROTHERO A. (1996), *Explosion assessment in confined vented geometries. SOLVEX large scale explosion tests and SCOPE model development*, Project report ref HSE Offshore Technology report – OTO 96004

CATES A., SAMUELS B. (1991), *A simple assessment methodology for vented explosions*, J. Loss Prev. Process ind., vol. 4, pp. 287-296

MOLKOV. V., EBER R.M., GRIGORASH A.V., TAMANINI F., DOBASHI R (2003), *Vented gaseous deflagrations: modeling of translating inertial vent covers*, J. Loss Prev. Process ind., vol. 16, pp. 395-402

JALLAIS S., (2013), *An inter-comparison exercise on CFD model capabilities to simulate hydrogen vented explosions*, ICHS Brussels

Van WINGERDEN C.J.M., ZEEUWEN J.P. (1983), *Venting of gas explosions in large rooms*, Proceedings of the 4th int. symp. On Loss Prevention and Safety Promotion in the Process Industries, IchemE series n°82, ISBN 085295 161 2

COOPER M.MG., FAIRWEATHER M., TITE P. (1986), *On the mechanisms of pressure generation in vented explosions*, Comb. and Flame, vol. 65, pp. 1-14

BIMSON S.J., BULL D.C., CRESSWELL T.M., MARKS P.R., MASTERS A.P., PROTHERO A., PUTTOCK J.S., ROWON J.J., SAMUELS B. (1993), *An experimental study of the physics of gaseous deflagration in a very large vented enclosure*, Proceedings

of the 14th International Colloquium on the Dynamics of Explosions and Reactive Systems, Coimbra, Portugal, August 1st-6th, 1993

CHOW S.K., CLEAVER R.P., FAIRWEATHER M., WALKER D.G. (2000), *An experimental study of vented explosions in a 3:1 aspect ratio cylindrical vessel*, TransIChemE, vol. 78, part B, pp425-433

HARRISON A.J., EYRE J.A. (1987), *"External Explosions" as a result of explosion venting*, Combustion Sci. and Tech. n°52, pp 91-106

CATLIN C.A. (1991), *Scale effects on the external combustion caused by venting of a confined explosion*, Comb. and Flame, vol. 83, pp. 399-411

PROUST C., LEPRETTE E. (2010), *The dynamics of vented gas explosions*., Process Safety Progress, vol. 29, pp. 231-235

BAUWENS C.R, DOROFEEV S.B.. (2014), *Effect of initial turbulence on vented explosion overpressures from lean hydrogen–air deflagrations*, International Journal of Hydrogen Energy Volume 39, Issue 35, 3 December 2014, Pages 20509-20515

Proust C, Jamois D, Hébrard H, Grégoire Y (2018), *Measuring the flow and the turbulence in dust air mixtures and in flames using a modified Mc Caffrey gauge*, Proceeding of International Symposium of Hazards, Protection, Mitigation of Industrial Explosion 2018, Kansas City

DUCLOS A., PROUST C., DAUBECH J., VERBECKE F. (2017), *Development of a realistic hydrogen flammable atmosphere inside a 4m3 enclosure*, Proceeding of International Conference of Hydrogen Safety, Hambourg 2017

KOROLL G.W., KUMAR R.K., BOWLES E.M. (1994), *Burning velocities of hydrogen-air mixtures*, Comb. and Flame, vol. 94, pp. 330-340

DAUBECH, J., PROUST, C., GENTILHOMME, O., JAMOIS C. and MATHIEU, L. (2013), *Hydrogen-Air vented EXPLOSIONS: new experimental data*, Proceeding of International Conference of Hydrogen Safety, San Fransisco 2013

DAUBECH J, (2008), *Contribution à l'étude de l'effet de l'hétérogénéité d'un prémélange gazeux sur la propagation d'une flamme dans un tube clos*, thèse de doctorat, Université d'Orléans

LEWIS B., Von ELBE G. (1987), *Combustion, flames and explosions of gases: 3rd edition*, Academic Press, London, ISBN 0-12-446751-2

BAUWENS C.R., CHAO J., DOROFEEV S.B., (2012), *Effect of hydrogen concentration on vented explosion overpressures from lean hydrogen–air deflagrations*, International Journal of Hydrogen Energy, Volume 37, Issue 22, November 2012, Pages 17599-17605